

1 A label-free, multiplex glycan microarray biosensor for influenza virus detection

2 Hanyuan Zhang,^{a,b} Alanna M. Klose,^b and Benjamin L. Miller^{a,b*}

3 ^aMaterials Science Program, University of Rochester, Rochester NY, USA 14627

4 ^bDepartment of Dermatology, University of Rochester Medical Center, Rochester NY, USA 14642

5 *Author to whom correspondence should be addressed: Benjamin_miller@urmc.rochester.edu

6 Abstract:

7 Newly emerging influenza viruses adapted from animal species pose significant pandemic
8 threats to public health. An understanding of hemagglutinin (HA)-receptor binding specificity to
9 host receptors is key to studying the adaptation of influenza viruses in humans. This information
10 may be particularly useful for predicting the emergence of a pandemic outbreak. Therefore, high-
11 throughput sensing technologies able to profile HA-receptor binding can facilitate studies of
12 influenza virus evolution and adaptation in humans. As a step towards this goal, we have prepared
13 glycan-based receptor analogue microarrays on the Arrayed Imaging Reflectometry (AIR)
14 platform. These arrays demonstrate label-free, multiplex detection and discrimination between
15 human and avian influenza viruses. Microarrays consisting of glycan probes with 2-6 and 2-3
16 linkages were prepared. After first confirming their ability to capture lectins (carbohydrate-binding
17 proteins) with known specificities, we observed that the arrays were able to discriminate between
18 and quantify human pandemic influenza A/California/07/2009 (H1N1pdm) and avian
19 A/Netherlands/1/2000 (H13N8) influenza viruses, respectively. As the method may be expanded
20 to large numbers of glycans (> 100) and virus subtypes (H1-H18), we anticipate it can be applied
21 to systematically evaluate influenza virus adaptation in humans. In turn, this will facilitate global
22 influenza surveillance and serve as a new tool enabling health organizations, government, research
23 institutes, and laboratories to react quickly in the face of a pandemic outbreak.

24

25 Keywords: Interferometry, microarray, glycan, influenza, receptor mimic, label-free sensing,
26 reflectometry, glycan conjugation

27

28

29

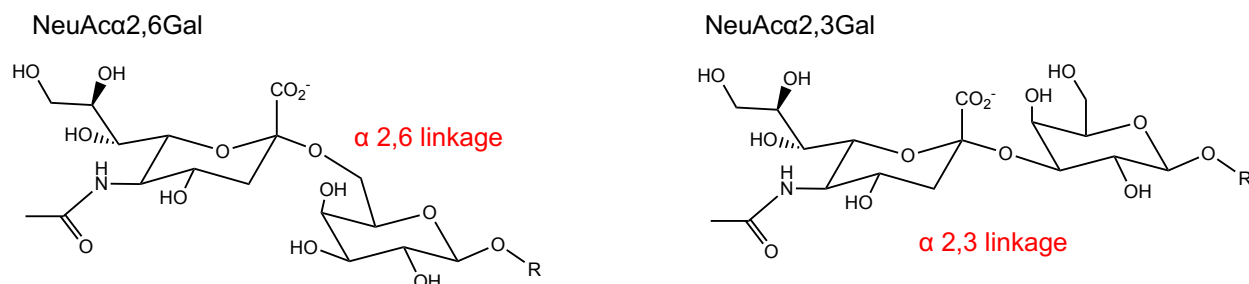
30

31 Introduction

32 The recent global outbreak of SARS-CoV-2 has resulted in dramatic social upheaval,
33 clearly highlighting the potential of an animal-sourced respiratory pathogen to rapidly produce
34 sustained human to human spread, with concomitant fatalities and significant economic damage.¹
35 Influenza virus, which possesses high mutation rates and adaptive abilities in different hosts and
36 has caused both historically significant pandemics as well as seasonal infections,^{2,3} requires
37 continuing attention to its antigenic evolution and adaptation in humans. Since the early years of
38 the last century, three hemagglutinin (HA) subtypes (H1, H2, and H3) and two neuraminidase (NA)
39 subtypes (N1, and N2) have adapted from animal species to enable circulation among humans.⁴
40 As a result, four significant influenza pandemics have occurred worldwide (1918 H1N1, 1957
41 H2N2, 1968 H3N2, and 2009 H1N1), resulting in millions of deaths and countless financial and
42 social costs.^{5,6,7,8} Since then, new animal-sourced influenza viruses including avian H5N1, H7N9,
43 and H9N2 strains have occasionally infected humans, but fortunately have not been able to
44 spread.^{9,10,11} However, further evolution of these viruses including gene reassortment events could
45 lead to their full adaptation to humans with high and sustained transmission ability. In particular,
46 the Asian lineage avian influenza H7N9 virus has achieved the largest spread, with 1,567
47 laboratory-confirmed human infections since it first emerged in 2013.^{12,13} This has further raised
48 the concern that an animal sourced influenza virus could trigger a pandemic outbreak.

49 Since HA-receptor specificity is a key factor in the process of infection, transmission and
50 adaptation of influenza viruses, many studies have focused on understanding the influence of
51 linkage structures of sialic acid groups in host receptor complex glycans, as these vary from species
52 to species.¹⁴ Human-adapted influenza HA proteins have a binding preference for α 2,6 linked
53 sialic acid moieties (N-acetylneuraminic acid, α 2,6, Galactose: abbreviated as NeuAc α 2,6Gal,
54 Figure 1), which are mostly found on the epithelial cells of the human upper respiratory tract.¹⁵ In
55 contrast, animal influenza HA proteins target the α 2,3 linked sialic acid moieties (NeuAc α 2,3Gal),
56 which are abundant in the epithelial cells of the intestine and the whole respiratory tract of birds
57 and other animals.¹⁶ Many studies have demonstrated that this difference in the linkage structures
58 of both sialic acids (α 2,6 vs. α 2,3), although seemingly subtle, thus determines the ability of
59 influenza viruses to infect different species.^{17,18} While PCR is the gold-standard diagnostic
60 technique for the presence of influenza virus, PCR cannot *a priori* determine the receptor-binding
61 specificity of an isolated influenza virus. Therefore, sensors for rapidly identifying the HA-

62 receptor specificity, and especially discrimination of influenza HA proteins binding α 2,6 and α 2,3
 63 linked sialic acids, are critical for assessing the adaptative ability of newly emerging animal
 64 influenza viruses. Such tools could facilitate the early prevention of potential influenza pandemics
 65 via rapid characterization of viral isolates.¹⁹



67 Figure 1: The structures of human and avian cell surface sialyloligosaccharides.
 68

69 The availability of synthetic glycans in different formats has led to their extensive
 70 application in microarray platforms.^{20, 21, 22} These synthesized glycans or “receptor binding
 71 analogues” can be immobilized on substrates for characterization of influenza virus specificity at
 72 varying levels of throughput.²³ In particular, microarrays developed by the Consortium for
 73 Functional Glycomics (CFG)²⁴ include several hundred covalently immobilized glycans ranging
 74 in size and functionality, thus offering the opportunity to systematically investigate the influenza
 75 HA specificity to a large number of glycans. However, methods used to evaluate influenza HA-
 76 glycan binding have primarily employed an ELISA-type format, with multistep workflows and
 77 fluorescent reporter reagents. Although some label-free biosensing technologies have been applied
 78 to measure binding avidity of HAs to glycan analogues, as far as we are aware none have been
 79 implemented in a multiplex format.^{25,26,27} Therefore, label-free sensor technologies able to rapidly
 80 profile influenza HA-glycan binding specificity in a microarray format are highly desirable.

81 To address this need, we have prepared and tested microarrays of influenza receptor
 82 binding analogues on the Arrayed Imaging Reflectometry (AIR) sensor platform. AIR is a label-
 83 free, multiplex detection solution. The platform utilizes a single-camera interferometric imaging
 84 setup, in which s-polarized light from a HeNe laser (632.8 nm) is expanded and collimated to
 85 illuminate arrays prepared on silicon / silicon oxide substrates. The reflected image of the array is
 86 captured by a charge-coupled device (CCD) camera. The thickness of the chips and microarrayed
 87 biomolecules is controlled precisely in order to create a near-perfect antireflection condition in the

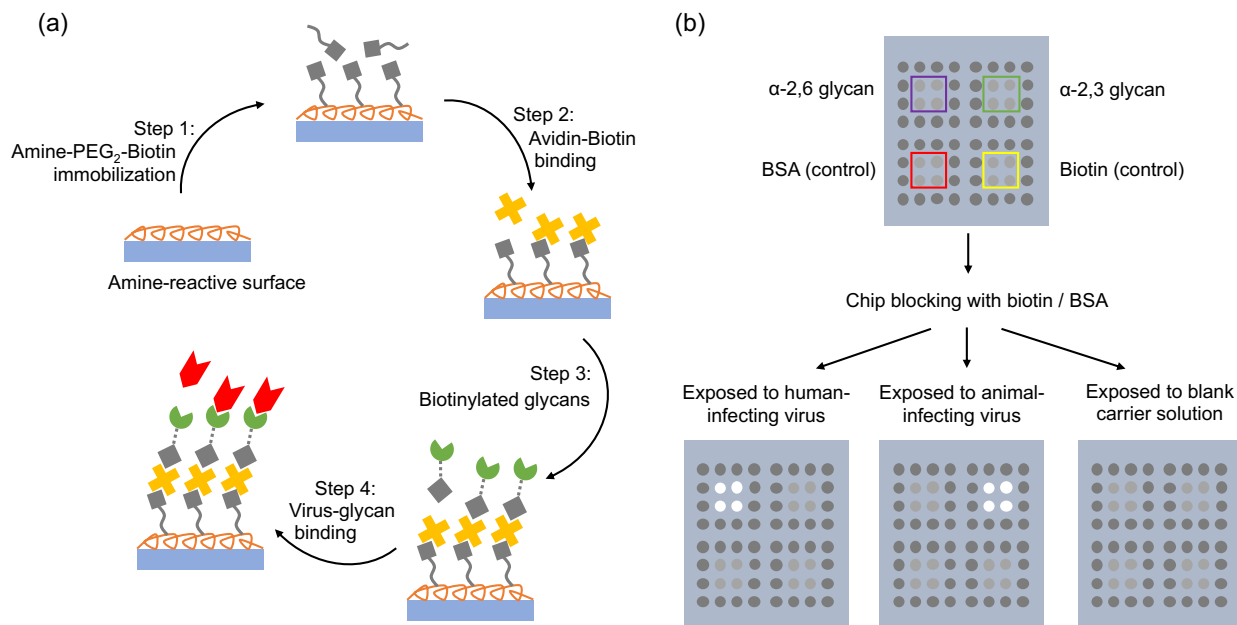
88 absence of target molecule binding.²⁸ Binding of the analyte of interest to a capture spot results in
89 a thickness change that perturbs the antireflection condition, resulting in light reflecting in
90 proportion to the amount of material captured. The utility of AIR has been demonstrated in a broad
91 range of applications, including detection and quantification of cytokines and other inflammatory
92 biomarkers in human serum,²⁹ antibodies to human autoantigens,³⁰ and as a real-time method for
93 monitoring protein-RNA binding.³¹ Recently, we have also used the technique as a method for
94 analyzing the human response to SARS-CoV-2 (COVID-19) infection.³²

95 In the context of influenza, we have used arrays of hemagglutinins (HAs) to monitor the
96 human³³ and avian³⁴ immune response to influenza infection or vaccination with AIR. AIR
97 microarray biosensors consisting of a library of vaccine derived human monoclonal antibodies (up
98 to 115-plex) have proven useful for serotyping influenza virus subtypes, and showed the potential
99 of systematically mapping the antigenic binding epitopes based on the array's response
100 patterns.^{35,36,37} To extend the methodology to HA receptor binding, we report here a glycan-based
101 AIR biosensor with α 2,6 and α 2,3 linked sialic acid polymeric receptor binding analogues. This
102 array is able to bind and discriminate between human- and avian-infectious influenza viruses. In
103 addition to demonstrating the first use of carbohydrate capture molecules on the AIR platform, this
104 work provides proof-of-concept for multiplex AIR arrays to help increase our understanding of
105 influenza biology, particularly to promote the prediction of viral adaptation across species.

106 **Results**

107 The workflow of microarray chip preparation and polymer-based glycan-antigen detection
108 is illustrated in Figure 2(a). A stable biotin-avidin layer was first prepared on the amine-reactive
109 Silicon/SiO₂ chips to enable immobilization of the biotinylated glycan probes.³⁸ The commercial
110 glycan receptor analogues are synthesized on a polyacrylamide (PAA) polymer carrier; this acts
111 as a spacer between the sensing surface of the chip and sialic acid moieties, limiting steric
112 interactions with the surface and enabling unbiased interactions.³⁹ Because AIR is an
113 interferometric method rather than a technique reliant on an evanescent field (as surface plasmon
114 resonance is, for example), use of a linker does not decrease detection sensitivity. Figure 2(b)
115 shows the microarray layout. To complement α 2,6 linked glycan (purple boxed) and α 2,3 linked
116 glycan (green boxed) probe spots, biotinylated bovine serum albumin (b-BSA) (red boxed) and
117 biotin (yellow boxed) spots were used at the lower sections as on-chip controls for nonspecific
118 binding. In addition, twelve replicate spots of biotinylated polyacrylamide carbohydrate probes

119 lacking sialic acid (galactose-beta-1,4-N-acetylglucosamine-beta-polyacrylamide-biotin, Galb1-
 120 4GlcNAcb-PAA-biotin) were printed surrounding each sub-section of the microarray to correct
 121 for any local changes in chip thickness. Prior to assay, the chips were blocked first with 0.1 mg/mL
 122 D-biotin solutions in PBS buffer and then BSA in sodium acetate. The prepared and blocked chips
 123 were then exposed to target protein or virus for the next steps. Control experiments used blank
 124 carrier solutions lacking the target antigen.



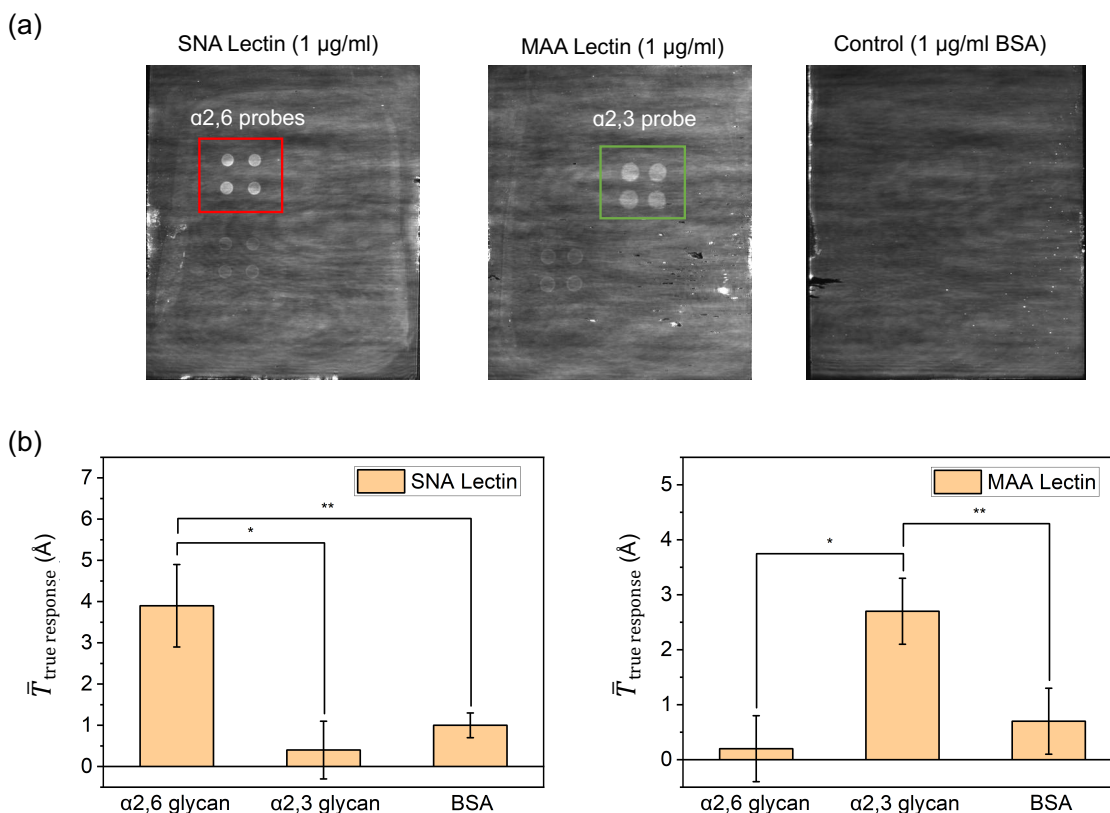
125
 126 Figure 2: (a) Schematic of AIR microarray chip preparation and incubation for virus-glycan
 127 binding detection. An amine-reactive chip surface is first uniformly coated with amine-PEG₂-
 128 biotin (Step 1), then avidin (Step 2) and stabilized. Biotinylated glycans are spotted (Step 3)
 129 completing the sensor manufacturing process. Incubation with virus (Step 4) constitutes the
 130 assay itself. (b) Layout design of receptor analogue glycan microarrays and response patterns for
 131 the discrimination of human-infecting (α 2,6-sialic acid binding) and avian-infecting (α 2,3-sialic
 132 acid binding) influenza viruses.

133
 134 To confirm that glycans immobilized on the array retain their expected specificity, we first
 135 tested binding of glycan-binding proteins (lectins). *Sambucus nigra* (SNA) and *Maackia*
 136 *amurensis* (MAA) lectin proteins are known to be specific for binding α 2,6 and α 2,3 linked glycans,
 137 respectively.^{40,41} Figure 3(a) shows experimental results for the discrimination of SNA and MAA
 138 lectin proteins spiked in the PBS solution at a concentration of 1 μ g/ml. The highlighted bright

139 spots (red boxed) in the AIR image for SNA lectin detection demonstrate a positive response of
140 the α 2,6 linked glycan probe spots. The α 2,3 linked glycan probe spots are muted indicating that
141 the SNA lectin proteins were selectively captured by α 2,6 linked glycan probe spots. In contrast,
142 the highlighted spots (green boxed) in the AIR image for target MAA lectin protein demonstrates
143 a strong positive response of only α 2,3 linked glycan probes, while the α 2,6 linked glycan probes
144 are muted. In addition, the overall probe morphologies of the AIR images are uniform, with no
145 “coffee ring” artifacts. This indicates that the surface chemistry and immobilization protocols
146 behave as desired.

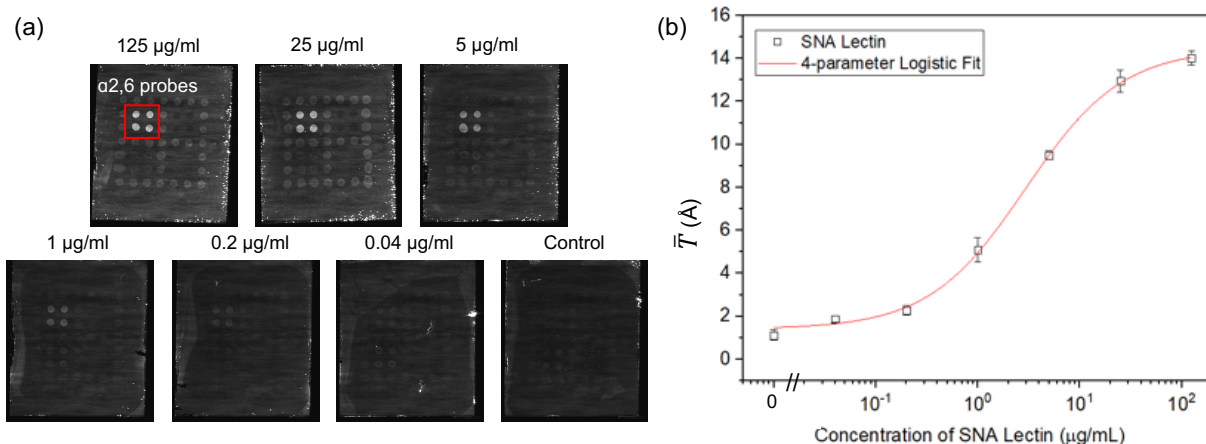
147 AIR microarray images also provide quantitative information regarding the binding affinity
148 and the amount of captured target. In Figure 3(b), the quantitative response data represented by the
149 increase of the thickness (in Å) of the captured materials on the microarray confirm the qualitative
150 observations from Figure 3(a). Differences between the positive responses of the α 2,6 linked
151 glycan probe spots and the negative responses of α 2,3 linked glycan probe spots were statistically
152 significant, with p-values of 0.009 (< 0.05) for SNA detection and 0.007 (< 0.05) for MAA
153 detection. Nonspecific binding to the b-BSA probe spots was also significantly lower than to
154 positive probe spots (both p-values are $0.002 < 0.05$). These results confirm the high selectivity of
155 the glycan microarrays for their specific lectin proteins.

156



157
 158 Figure 3: (a) AIR microarray images (250 ms exposure) of $\alpha 2,6$ linked, $\alpha 2,3$ linked, b-BSA and
 159 biotin probe spots for the discrimination of SNA and MAA lectin proteins. (b) Quantitative
 160 results of the microarray response against SNA and MAA lectin proteins.

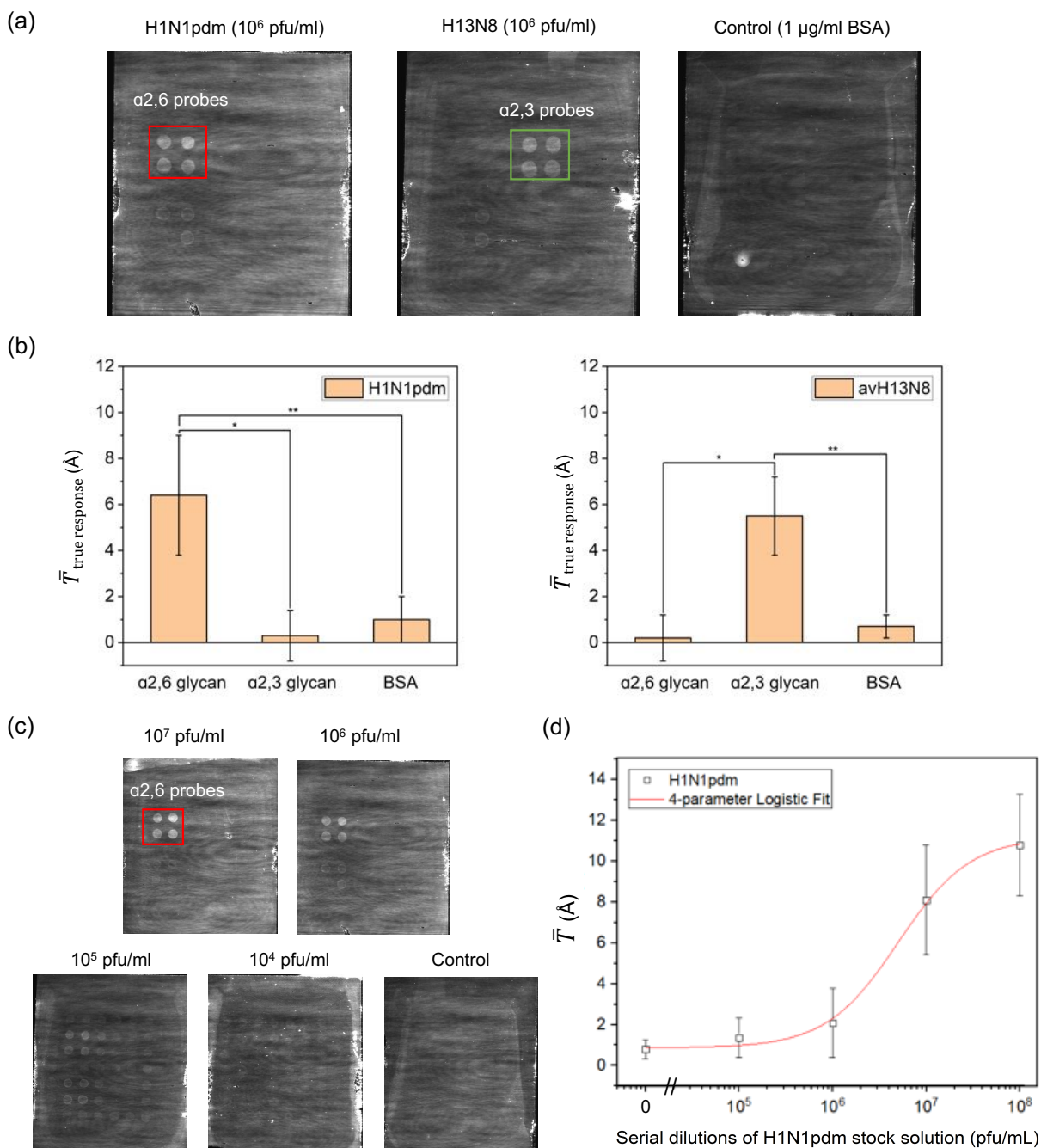
161
 162 To confirm that lectin binding to the array was analytically well behaved, we tested the
 163 response of microarrays exposed to a serial dilution of SNA lectin protein in PBS. The response
 164 data of the $\alpha 2,6$ linked glycan probe spots (red boxed) in Figure 4(a) following exposure to
 165 concentrations of SNA ranging from 0.04 to 125 $\mu\text{g/ml}$ are plotted in Figure 4(b). A concentration-
 166 dependent 4-parameter logistic equation was used to fit the data, yielding an adjusted R-square
 167 value of 0.99. The limit of detection, defined based on three times the standard deviation of the
 168 lowest measurement, was found to be 0.06 $\mu\text{g/ml}$ with a 95% confidence interval. This provides
 169 an overall detection range of 4 logs in concentration. The overall response curve and observed
 170 SNA binding affinity are similar to previously published single-channel SPR data for SNA lectin
 171 binding an immobilized $\alpha 2,6$ sialoside.⁴⁰



172
 173 Figure 4: (a) AIR microarray images (100 ms exposure) following exposure to serial dilutions of
 174 SNA lectin protein. (b) Concentration-dependent response data for SNA lectin binding to the
 175 array. The red line is a 4-parameter logistic fit of the response at each concentration (adjusted R-
 176 Square: 0.99).

177
 178 To assess the ability of the glycan-based microarray biosensor to detect and discriminate
 179 live human and avian influenza viruses, we incubated the microarrays with selected pseudotyped
 180 influenza viruses spiked at 10⁶ pfu/mL in 10% FBS solutions overnight, and measured the probe
 181 responses relative to the control chips. Pseudotyped, or single-cycle, infectious influenza A viruses
 182 are recombinant strains in which the hemagglutinin (HA) gene is deleted or replaced with a
 183 fluorescent marker such as GFP or mCherry.⁴² As such, they can only replicate when co-
 184 transfected with an HA expressing plasmid, and are therefore safe to handle in the laboratory at a
 185 low biosafety level. Results for these experiments are shown in Figure 5. Human influenza
 186 H1N1pdm bound to the α2,6 linked glycan probe spots with high selectivity, as expected for this
 187 virus. Likewise, avian influenza H13N8 virus only bound to the α2,3 linked glycan probe spots,
 188 consistent with its species specificity. In both cases, the microarray response image obtained from
 189 exposure to 1 µg/ml of BSA spiked in 10% FBS solution was used as the control. Quantified
 190 response data (Figure 5(b)) confirms specific binding of virus to each glycan probe for human (red
 191 boxed) and avian (green boxed) influenza viruses, respectively. Significant differences between
 192 the binding responses of the analyte probe spots and the control groups were obtained, with p-
 193 values of 0.029 (< 0.05) for human H1N1pdm influenza virus and 0.012 (< 0.05) for avian H13N8
 194 influenza virus.

195 The dynamic range of the glycan microarray was also tested via exposure to serial dilutions
196 of the human influenza H1N1pdm virus stock (10^8 pfu/mL) spiked in 10% FBS. The AIR
197 microarray images were captured (Figure 5(c)), recorded and analyzed for quantitative responses
198 as shown in the Figure 5(d). Each probe spot (red boxed) was further resolved for estimating the
199 bound human H1N1pdm virus. Analysis of the resulting response curve indicates a lower limit of
200 detection of 9.29×10^5 pfu/mL, or a three order of magnitude dynamic range for detection. This is
201 an order of magnitude lower than that observed for SNA lectin, and is a direct result of the
202 increased standard deviations observed for each virus concentration. Further optimization of the
203 assay protocol may allow for improvement in both the detection limit and dynamic range. However,
204 we note that the observed performance is more than sufficient to enable discrimination of binding
205 to different receptor glycan analogues (as in Figure 5a), the primary goal for the assay.



206

207

208 Figure 5: Responses of the AIR glycan microarray to human influenza H1N1pdm and avian

209

influenza H13N8 viruses. (a) Images for arrays exposed to H1N1pdm (left), H13N8 (center), and

210

a control sample (right). (b) Quantitative response data of the glycan microarray to human

211

influenza H1N1pdm virus (left) and avian influenza H13N8 virus (right). (c) AIR images (250

212

ms exposure) show chip response in (d) at varying concentrations of virus.

213

214 **Discussion**

215 The prevention of influenza pandemics is a significant endeavor that requires close and
216 efficient collaboration across broad scientific fields including bioengineering, immunology,
217 virology, bioinformatics, and medicine. Influenza pandemics usually originate from an animal-
218 sourced virus that has acquired the ability of consistent transmission among humans. In the fight
219 against such an outbreak, time is a very limited commodity. Currently, the front line of a pandemic
220 is defended by health organizations and governments which provide strategies for developing
221 vaccines and treatment guidelines. However, the lengthy process of producing effective vaccines
222 can delay resolution of the pandemic, resulting in significant casualties. Our previous work used
223 an antibody microarray biosensor to demonstrate an effective strategy for responding quickly to
224 an emerging pandemic outbreak by identifying known antigenically similar vaccine strains of
225 influenza to facilitate the vaccine discovery process.³⁶ This approach was further tested and found
226 to be useful in a national (USA) mock pandemic exercise.³⁷ The work described here is intended
227 to enable the identification of human-infecting (and potentially pandemic) virus strains as they
228 evolve from an animal source before they become pandemic, thereby allowing a public health
229 response at an even earlier time point.

230 To that end, we have successfully demonstrated glycan-based microarray biosensors on the
231 AIR platform that easily and effectively discriminates between animal- and human-infective
232 influenza viruses based on their HA-receptor glycan specificity. Microarrays with immobilized 2-
233 6 and 2-3 linked glycan analogues were capable of label-free and multiplex detection of glycan-
234 binding lectin proteins, and discrimination between the human influenza A/California/07/2009
235 H1N1pdm strain and avian sourced influenza A/Netherlands/1/2000 H13N8 virus. We observed
236 an unoptimized lower limit of detection of 0.06 $\mu\text{g/ml}$ for the lectins, and arrays were analytically
237 well behaved, exhibiting a concentration dependent response consistent with Langmuir binding
238 behavior. The unoptimized detection limit for H1N1pdm virus was 9.29×10^5 pfu/mL. While
239 optical sensors have been described with single-particle detection sensitivity for influenza,⁴³ our
240 observed sensitivity is more than sufficient for the envisioned application. AIR provides several
241 advantages over traditional immunoassay formats such as ELISA including a much simpler
242 workflow. As a multiplex technique, AIR provides much higher data throughput than either
243 singleplex ELISA or single-channel surface plasmon resonance (SPR) assays, with comparable or

244 better sensitivity. Finally, since the performance of AIR is independent of plex (i.e. the number of
245 different analytes captured on the array), we expect that it will be straightforward to expand this
246 microarray to large numbers of glycans for systematically investigating the receptor specificity of
247 influenza subtypes from many different species. Such an array will significantly facilitate global
248 virus surveillance and efforts to prevent future outbreaks of pandemic influenza.

249 **Materials and Methods**

250 **Materials and reagents**

251 Amine-reactive AIR substrates (5 × 6 mm) were purchased from Adarza BioSystems, Inc.
252 D-biotin and EZ-Link amine-PEG₂-biotin were purchased from ThermoFisher Scientific. Avidin
253 was purchased from Rockland Immunochemicals, Inc. Pseudotyped influenza viruses
254 (A/California/07/2009 H1N1pdm and avian A/Netherlands/1/2000 H13N8) were a gift of Prof.
255 Luis Martinez-Sobrido, and prepared as previously described.⁴⁴ Biotinylated polyacrylamide
256 (PAA) carbohydrate molecules (3'-Sialyllactose-PAA-biotin 01-038, 6'-Sialyllactose-PAA-biotin
257 01-039, and Galb1-4GlcNAcb-PAA-biotin 01-022) were purchased from GlycoTech. Biotinylated
258 bovine serum albumin (b-BSA) was purchased from Rockland Immunochemicals, Inc. Fetal
259 bovine serum (FBS) was purchased from Gibco by ThermoFisher Scientific.

260 **Chip preparation and functionalization**

261 First, amine-reactive silicon/SiO₂ chips were incubated with amine-PEG₂-biotin (1 mg/ml)
262 in 1× PBS solution (PBS: 137 mM NaCl, 2.7 mM KCl, 10 mM Na₂HPO₄, and 1.76 mM KH₂PO₄-
263 H₂O, pH 7.4) overnight, with agitation on a rotating platform shaker, at room temperature. Next,
264 chips were washed in Assay Wash Buffer (AWB: mPBS (150 mM NaCl, 10 mM Na₂HPO₄, 10
265 mM NaH₂PO₄) with 0.005% tween-20, pH 7.2) for 5 minutes before incubation in 40 µg/mL avidin
266 in PBS for 1 hour, shaking, at room temperature. After batch-rinsing the chips for 5 minutes in
267 AWB, they were incubated in a 1% solution of StabilCoat Plus[®] in 18 MΩ-cm water produced by
268 a Barnstead Nanopure II purification system (Nanopure[™]) for 20 minutes before being spun dry
269 for 1 minute at 500 RPM after being attached to the rotating platform of a wafer polisher (Ecomet
270 4, Buehler, IL, USA).

271 Biotinylated polymer-based carbohydrate probes were suspended at a concentration of 250
272 µg/mL in 10 mM phosphate-buffered saline (PBS) at pH 7.0. Prepared probe solutions were
273 spotted at a droplet volume of 250 pL using a piezoelectric arrayer (Sciencion S3). Four replicate

274 spots were printed for each type of carbohydrate probe. Twelve replicate spots of carbohydrate
275 probes lacking the sialic acid moiety were printed adjacent to and surrounding each group of probe
276 spots as negative controls for nonspecific binding and intra-chip thickness variation. Biotinylated
277 BSA (250 $\mu\text{g}/\text{mL}$) and D-biotin (1 mg/mL) solutions prepared in PBS were also printed on the
278 array in order as negative controls. All spots were printed with a center-to-center distance of 300
279 μm .

280 **Assay protocols**

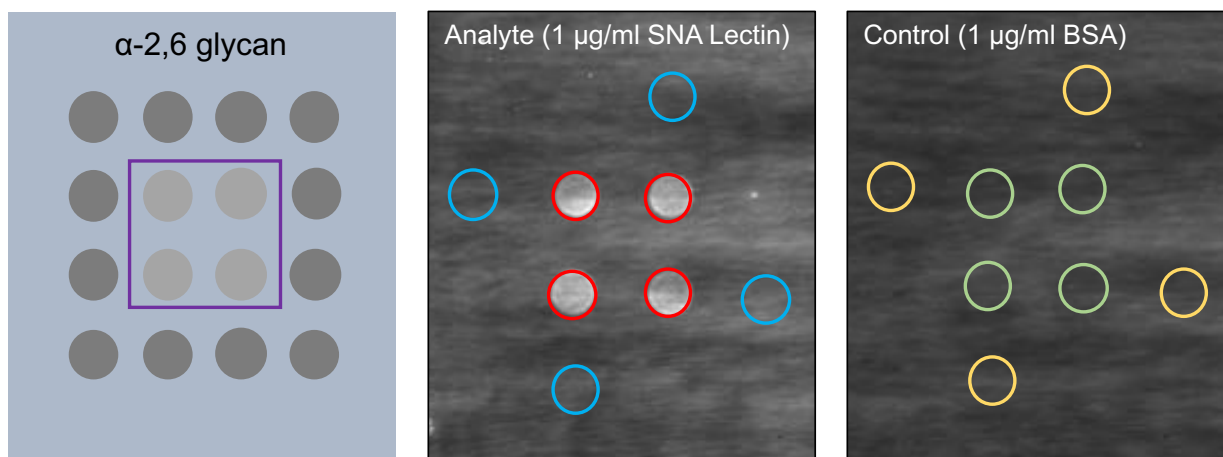
281 Experiments with glycan-binding lectin proteins (used to confirm the specificity of
282 immobilized probes) and pseudotyped influenza viruses followed the same general procedure.
283 Two blocking solutions consisting of (1) 0.1 mg/mL D-biotin in 10 mM PBS and (2) 10 mg/mL
284 BSA in sodium acetate buffer (50 mM at pH 5.0) were prepared and added to separate rows of a
285 96-well plate. After being incubated in BSA blocking solutions, the chips were washed in modified
286 PBS-EDTA-Tween 20 (10 mM PBS, 5 mM EDTA, and 0.5% Tween 20 at pH 7.4) assay wash
287 buffer (AWB) thoroughly and then transferred into a BSA preblocked row for target exposure.
288 Solutions of lectin proteins were prepared at a concentration of 1 $\mu\text{g}/\text{mL}$ in PBS. Viral titers of
289 human and avian pseudotyped influenza viruses were reconstituted to 10^6 plaque forming units
290 (pfu)/ mL in 10% FBS solutions for target exposure, or serially diluted in 10% FBS from a 10^8
291 pfu/ mL stock. Blank 10% FBS solutions were used as negative control groups. Three chips were
292 used per condition and incubated overnight at room temperature. After incubation, all chips were
293 washed in AWB several times and rinsed in deionized, glass-distilled water. Finally, chips were
294 dried under a stream of nitrogen gas prior to imaging.

295 **Data acquisition and analysis**

296 Dried chips were imaged immediately on a prototype AIR reader (Adarza BioSystems,
297 Inc.). AIR images were acquired in a 16-bit TIFF format with an exposure time of 100 ms or 250
298 ms for lectin detection and 250 ms for virus detection. Optimal exposure time is dictated by the
299 concentration of the analyte. At low concentration, sensitivity may be enhanced by increasing the
300 exposure time, while at high concentration, shorter exposures are often required to prevent
301 saturation of the detector. Multiple exposures may be obtained for each sample if desired. The AIR
302 images were then analyzed using NIH-ImageJ (version 1.46r). Where necessary, contrast
303 enhancement was used to locate spots; all quantitative data was obtained from un-altered images.
304 Final plots and 4-parameter logistic regression fits were generated in OriginPro 2020 (OriginLab

305 Corporation). The response of the biotinylated glycan probes lacking sialic acid moieties was used
 306 as a control for nonspecific binding to determine the true response data of the other probe spots.
 307 For each array spot, the response values were calculated by converting the reflection intensity unit
 308 to thickness based on an experimentally derived reference response model.^{28,36} The reference
 309 response model plots the relationship between reflected intensities acquired for different exposures
 310 (100 to 500 ms) and their corresponding thicknesses as measured by ellipsometry. For each spot,
 311 a median value was obtained from the histogram of the pixel intensities measured by ImageJ, and
 312 then four median values of the four replicate spots of the same probe were averaged and used as
 313 the true response data after correcting for the response of the control chip. This procedure is
 314 illustrated in Figure 6, using a chip carrying the α 2,6 glycan analogue and incubated with SNA
 315 lectin (discussed further below) as an example. A two-sample t test was applied to analyze the
 316 response data and a P-value cutoff of 0.05 was used to evaluate the significance of the differences
 317 between positive and negative groups. The standard deviations of replicate spots for each analyte
 318 concentration of both control and analyte chips were used to determine the error bars. All
 319 experiments were repeated twice to confirm observations.

320



$$\bar{T}_{analyte} = \frac{\sum_{i=1}^n (x_i - \bar{c})}{n}$$

$$\bar{T}_{control} = \frac{\sum_{i=1}^n (x_i - \bar{c})}{n}$$

$$\bar{T}_{true\ response} = \bar{T}_{analyte} - \bar{T}_{control}$$

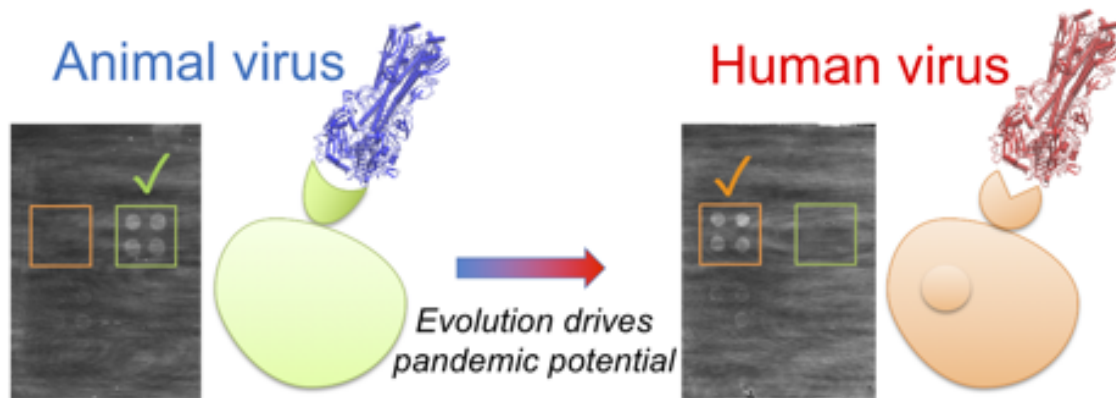
321

322 Figure 6: Analysis protocol for AIR images. \bar{T}_{analyte} is the average corrected analyte probe
323 thickness, \bar{T}_{control} is the average corrected control probe thickness, x is the median intensity
324 converted thickness of a single test probe, \bar{c} is the average median intensity-converted-thickness
325 of a four replicate correction probes surrounding each test probe, and n is the number of test
326 probes. A contrast-enhanced image was used to locate the spots in the control.

327
328

329 Acknowledgement. We thank Prof. Luis Martínez-Sobrido for generously donating pseudotyped
330 influenza viruses. This project has been funded in whole or in part with Federal funds from the
331 National Institute of Allergy and Infectious Diseases, National Institutes of Health, Department of
332 Health and Human Services, under CEIRS Contract No. HHSN272201400005C.

333
334 TOC Image:



335
336

337 **References**

- ¹ COVIDView Weekly Summary Updated August 14, 2020, Centers for Disease Control and Prevention (CDC). <https://www.cdc.gov/coronavirus/2019-ncov/covid-data/covidview/index.html>. Accessed August 16, 2020.
- ² Webster, R. G., Bean, W. J., Gorman, O. T., Chambers, T. M., Kawaoka, Y. (1992) Evolution and ecology of influenza A viruses. *Microbiological reviews* 56, 152-179.
- ³ Taubenberger, J. K., Kash, J. C. (2010) Influenza virus evolution, host adaptation, and pandemic formation. *Cell host & microbe* 7, 440-451.
- ⁴ Neumann, G., Kawaoka, Y. (2006) Host range restriction and pathogenicity in the context of influenza pandemic. *Emerging infectious diseases* 12, 881.
- ⁵ Reid, A. H., Fanning, T. G., Hultin, J. V., Taubenberger, J. K. (1999) Origin and evolution of the 1918 “Spanish” influenza virus hemagglutinin gene. *Proceedings of the National Academy of Sciences* 96, 1651-1656.
- ⁶ Joseph, U., Linster, M., Suzuki, Y., Krauss, S., Halpin, R. A., Vijaykrishna, D., Fabrizio, T. P., Bestebroer, T. M., Maurer-Stroh, S., Webby, R. J., et al. (2015) Adaptation of pandemic H2N2 influenza A viruses in humans. *Journal of Virology* 89, 2442.
- ⁷ Kilbourne, E. D. (2006) Influenza pandemics of the 20th century. *Emerging infectious diseases* 12, 9.
- ⁸ Al-Muharri, Z. (2010) Understanding the influenza A H1N1 2009 pandemic. *Sultan Qaboos University medical journal* 10, 187-195.
- ⁹ Claas, E. C., Osterhaus, A. D., Van Beek, R., De Jong, J. C., Rimmelzwaan, G. F., Senne, D. A., Krauss, S., Shortridge, K. F., Webster, R. G. (1998) Human influenza A H5N1 virus related to a highly pathogenic avian influenza virus. *The Lancet* 351, 472-477.
- ¹⁰ Gao, R., Cao, B., Hu, Y., Feng, Z., Wang, D., Hu, W., Chen, J., Jie, Z., Qiu, H., Xu, K., et al. (2013) Human infection with a novel avian- origin influenza A (H7N9) virus. *New England Journal of Medicine* 368, 1888-1897.
- ¹¹ Peiris, M., Yuen, K., Leung, C., Chan, K., Ip, P., Lai, R., Orr, W., Shortridge, K. (1999) Human infection with influenza H9N2. *The Lancet* 354, 916-917.
- ¹² Kile, J. C., Ren, R., Liu, L., Greene, C. M., Roguski, K., Iuliano, A. D., Jang, Y., Jones, J., Thor, S., Song, Y. (2017) Update: increase in human infections with novel Asian lineage avian influenza A (H7N9) viruses during the fifth epidemic-China, October 1, 2016-August 7, 2017. *MMWR. Morbidity and mortality weekly report* 66, 928-932.

- ¹³ Human infection with avian influenza A(H7N9) virus – China: Update, September 5, 2018. <https://www.who.int/csr/don/05-september-2018-ah7n9-china/en/>, obtained August 14, 2020.
- ¹⁴ Weis, W., Brown, J. H., Cusack, S., Paulson, J. C., Skehel, J. J., Wiley, D. C. (1988) Structure of the influenza virus haemagglutinin complexed with its receptor, sialic acid. *Nature* 333, 426-431.
- ¹⁵ Matrosovich, M. N., Matrosovich, T. Y., Gray, T., Roberts, N. A., Klenk, H.-D. (2004) Human and avian influenza viruses target different cell types in cultures of human airway epithelium. *Proceedings of the National Academy of Sciences* 101, 4620-4624.
- ¹⁶ Shinya, K., Ebina, M., Yamada, S., Ono, M., Kasai, N., Kawaoka, Y. (2006) Avian flu: influenza virus receptors in the human airway. *Nature* 440, 435.
- ¹⁷ Viswanathan, K., Chandrasekaran, A., Srinivasan, A., Raman, R., Sasisekharan, V., Sasisekharan, R. (2010) Glycans as receptors for influenza pathogenesis. *Glycoconj J* 27, 561-570.
- ¹⁸ Byrd-Leotis, L., Jia, N., Dutta, S., Trost, J. F., Gao, C., Cummings, S. F., Brulke, T., Müller-Loennies, S., Heimbürg-Molinaro, J., Steinhauer, D. A., et al. (2019) Influenza binds phosphorylated glycans from human lung. *Sci Adv.* 13, eaav2554.
- ¹⁹ Taubenberger, J. K., Morens, D. M. (2008) The pathology of influenza virus infections. *Annual review of pathology* 3, 499-522.
- ²⁰ Stevens, J., Blixt, O., Paulson, J. C., Wilson, I. A. (2006) Glycan microarray technologies: tools to survey host specificity of influenza viruses. *Nature Reviews Microbiology* 4, 857.
- ²¹ Stevens, J., Blixt, O., Glaser, L., Taubenberger, J. K., Palese, P., Paulson, J. C., Wilson, I. A. (2006) Glycan microarray analysis of the hemagglutinins from modern and pandemic influenza viruses reveals different receptor specificities. *Journal of molecular biology* 355, 1143-1155.
- ²² de Paz, J. L., Seeberger, P. H. in *Carbohydrate Microarrays*. (Springer, 2012), pp. 1- 12.
- ²³ McQuillan, A. M., Byrd-Leotis, L., Heimbürg-Molinaro, J., Cummings, R. D. (2019) Natural and synthetic sialylated glycan microarrays and their applications. *Front. Mol. Biosci.* 6, 88.
- ²⁴ Blixt, O., Head, S., Mondala, T., Scanlan, C., Huflejt, M. E., Alvarez, R., Bryan, M. C., Fazio, F., Calarese, D., Stevens, J. (2004) Printed covalent glycan array for ligand profiling of diverse glycan binding proteins. *Proceedings of the National Academy of Sciences* 101, 17033-17038.
- ²⁵ Xiong, X., Martin, S. R., Haire, L. F., Wharton, S. A., Daniels, R. S., Bennett, M. S., McCauley, J. W., Collins, P. J., Walker, P. A., Skehel, J. J., et al. (2013) Receptor binding by an H7N9 influenza virus from humans. *Nature* 499, 496.

- ²⁶ Suenaga, E., Mizuno, H. Penmetcha, K. K. R. (2012) Monitoring influenza hemagglutinin and glycan interactions using surface plasmon resonance. *Biosensors and Bioelectronics* 32, 195-201.
- ²⁷ Fei, Y., Sun, Y. S., Fei, Y., Sun, Y. S., Li, Y., Yu, H., Lau, K., Landry, J. P., Luo, Z., Baumgarth, N., et al. (2015) Characterization of Receptor Binding Profiles of Influenza A Viruses Using An Ellipsometry-Based Label-Free Glycan Microarray Assay Platform. *Biomolecules* 5, 1480-1498.
- ²⁸ Mace, C. R., Striemer, C. C., Miller, B. L. (2006) Theoretical and experimental analysis of arrayed imaging reflectometry as a sensitive proteomics technique. *Anal. Chem.* 78, 5578-5583.
- ²⁹ Mace, C. R., Striemer, C. C., Miller, B. L. (2008) Detection of human proteins using arrayed imaging reflectometry. *Biosensors and Bioelectronics* 24, 334-337.
- ³⁰ Bucukovski, J., Carter, J. A., Striemer, C. C., Müllner, S., Schulte-Pelkum, J., Schulz-Knappe, P., Miller, B. L. (2018) Label-free microarray-based detection of autoantibodies in human serum. *Journal of Immunological Methods* 459, 44-49.
- ³¹ Yadav, A. R., Mace, C. R., Miller, B. L. (2014) Examining the interactions of the splicing factor MBNL1 with target RNA sequences via a label-free, multiplex method. *Anal. Chem.* 86, 1067-1075.
- ³² Steiner, D. J., Cognetii, J. S., Luta, E. P., Klose, A. M., Bucukovski, J., Bryan, M. R., Schmuke, J. J., Nguyen-Contant, P., Sangster, M. Y., Topham, D. J., et al. (2020) Array-based analysis of SARS-CoV-2, other coronaviruses, and influenza antibodies in convalescent COVID-19 patients. *Biosensors and Bioelectronics* 169, 112643.
- ³³ Mace, C. R., Topham, D. J., Mosmann, T. R., Quataert, S. A., Treanor, J. J., Miller, B. L. (2011) Label-free, arrayed sensing of immune response to influenza antigens. *Talanta* 83, 1000-1005.
- ³⁴ Bucukovski, J., Latorre-Margalef, N., Stallknecht, D. E., Miller, B. L. (2015) A multiplex label-free approach to avian influenza surveillance and serology. *PLoS ONE* 10, e0134484.
- ³⁵ Zhang, H., Dunand, C. H., Wilson, P. Miller, B. L. (2016) A label-free optical biosensor for serotyping “unknown” influenza viruses. *Proc. SPIE 9824, Chemical, Biological, Radiological, Nuclear, and Explosives (CBRNE) Sensing XVII*, 982405.
- ³⁶ Zhang, H., Henry, C. Anderson, C. S., Nogles, A., DeDiego, M. L., Bucukovski, J. Martinez-Sobrido, L., Wilson, P. C., Topham, D. J. Miller, B. L. (2018) Crowd on a chip: Label-free human monoclonal antibody arrays for serotyping influenza. *Anal. Chem.* 90, 9582-9590.
- ³⁷ Martienz-Sobrido, L., Blanco-Lobo, P., Rodriguez, L., Fitzgerald, T., Zhang, H., Nguyen, P., Anderson, C. S., Holden-Wiltse, J., Bandyopadhyay, S., Nogales, A., et al. (2020) Characterizing emerging canine H3 influenza viruses. *PLoS Pathogens* 16, e1008409.

- ³⁸ Klose, A.; Miller, B. L. (2020) A stable biotin-streptavidin surface enables multiplex, label-free protein detection by aptamer and aptamer-protein arrays using Arrayed Imaging Reflectometry *Sensors* *20*, 5745.
- ³⁹ Reimhult, E., Höök, F. (2015) Design of Surface Modifications for Nanoscale Sensor Applications. *Sensors* *15*, 1635-1675.
- ⁴⁰ Linman, M. J., Taylor, J. D., Yu, H., Chen, X., Cheng, Q. (2008) Surface plasmon resonance study of protein-carbohydrate interactions using biotinylated sialosides. *Anal. Chem.* *80*, 4007-4013.
- ⁴¹ Nicholls, J. M., Bourne, A. J., Chen, H., Guan, Y., Peiris, J. M. (2007) Sialic acid receptor detection in the human respiratory tract: evidence for widespread distribution of potential binding sites for human and avian influenza viruses. *Respiratory Research* *8*, 73.
- ⁴² Nogales, A., Baker, S. F., Domm, W., Martínez-Sobrido, L. (2016) Development and applications of single-cycle infectious influenza A virus (scIAV). *Virus Res.* *216*, 26-40.
- ⁴³ Vollmer, F., Arnold, S., Keng, D. (2008) Single virus detection from the reactive shift of a whispering-gallery mode. *Proceedings of the National Academy of Sciences* *105*, 20701-20704.
- ⁴⁴ Nogales, A., Baker, S. F., Martinez-Sobrido, L. (2015) Replication-competent influenza A viruses expressing a red fluorescent protein. *Virology* *476*, 206-216.